EBioMedicine 28 (2018) 251–260

Contents lists available at ScienceDirect

EBioMedicine

journal homepage: www.ebiomedicine.com

Research Paper

Chitinase-3-like Protein 1: A Progranulin Downstream Molecule and Potential Biomarker for Gaucher Disease

Jinlong Jian [a], Yuehong Chen [a], Rossella Liberti [a], Wenyu Fu [a], Wenhuo Hu [a], Rachel Saunders-Pullman [b], Gregory M. Pastores [c,1], Ying Chen [d], Ying Sun [e], Gregory A. Grabowski [e], Chuan-ju Liu [a,f,*]

[a] Department of Orthopaedic Surgery, New York University Medical Center, New York, NY, 10003, USA
[b] Department of Neurology, Mount Sinai Beth Israel Medical Center, New York, NY 10003, USA
[c] Department of Neurology, New York University School of Medicine, 550 First Ave, New York, NY 10016, USA
[d] Depression Evaluation Service, New York State Psychiatric Institute, 1051 Riverside Drive, New York, NY 10032, USA
[e] The Division of Human Genetics, Cincinnati Children's Hospital Medical Center, Cincinnati, OH 45229, USA
[f] Department of Cell Biology, New York University School of Medicine, New York, NY 10016, USA

ARTICLE INFO

Article history:
Received 2 January 2018
Received in revised form 20 January 2018
Accepted 20 January 2018
Available online 31 January 2018

Keywords:
Progranulin
Gaucher disease
Chitinase-3-like-1
Lysosomal storage diseases

ABSTRACT

We recently reported that progranulin (PGRN) is a novel regulator of glucocerebrosidase and its deficiency associates with Gaucher Diseases (GD) (Jian et al., 2016a; Jian et al., 2018). To isolate the relevant downstream molecules, we performed a whole genome microarray and mass spectrometry analysis, which led to the isolation of Chitinase-3-like-1 (CHI3L1) as one of the up-regulated genes in PGRN null mice. Elevated levels of CHI3L1 were confirmed by immunoblotting and immunohistochemistry. In contrast, treatment with recombinant Pcgin, a derivative of PGRN, as well as imigluerase, significantly reduced the expressions of CHI3L1 in both PGRN null GD model and the fibroblasts from GD patients. Serum levels of CHIT1, a clinical biomarker for GD, were significantly higher in GD patients than healthy controls (51.16 ± 2.824 ng/ml vs 35.07 ± 2.099 ng/ml, $p < 0.001$). Similar to CHIT1, serum CHI3L1 was also significantly increased in GD patients compared with healthy controls (1736 ± 152.1 pg/ml vs 684.7 ± 68.20 pg/ml, $p < 0.001$). Whereas the PGRN level is significantly reduced in GD patients as compared to the healthy control (91.56 ± 3.986 ng/ml vs 150.6 ± 4.501, $p < 0.001$). Collectively, these results indicate that CHI3L1 may be a previously unrecognized biomarker for diagnosing GD and for evaluating the therapeutic effects of new GD drug(s).

1. Introduction

Gaucher disease (GD), common lysosomal storage disease (LSD), is caused by mutations in *GBA1* with resultant defective glucocerebrosidase (GCase) activity and consequent accumulation of its substrate β-glucosylceramide (β-GlcCer) in macrophages and other cell types (Jian et al., 2016a). There are three types of GD based on its primary central nervous system (CNS) involvement: Type 1 does not manifest with early onset primary CNS disease and has previously been described as non-neuropathic. Patients with GD types 2 and 3 have primary CNS impairments. Type 2 features acute neuropathic disease of infancy. Type 3 is marked by chronic neuropathy with highly variable primary CNS onset and involvement. The peripheral manifestations of GD include hepatosplenomegaly and pancytopenia, due to bone marrow infiltration and splenic sequestration. Although *GBA1* mutations are the primary cause of GD, there is broad heterogeneity in clinical manifestations even among patients carrying the same *GBA1* mutations, ranging from very early disease onset to very mild clinical presentations (Biegstraaten et al., 2011; Elstein et al., 2010). These diverse variations are not directly attributable to different *GBA1* mutations and may relate to unidentified modifier genes.

PGRN is also known as granulin–epithelin precursor (GEP) (Zanocco-Marani et al., 1999), proepithelin (PEPI) (Shoyab et al., 1990; Plowman et al., 1992), acrogranin (Anakwe and Gerton, 1990), and GP88/PC-cell derived growth factor (PCDGF) (Zhou et al., 1993). PGRN is a growth factor with multiple functions, including promoting cell proliferation, stimulating wound healing (Zhao and Bateman, 2015; He et al., 2003) and regulating immune response (Fu et al., 2016; Jian et al., 2013a; Jian et al., 2018; Liu et al., 2014; Liu and Bosch, 2012; Mundra et al., 2016; Wei et al., 2014a; Wei et al., 2016; Williams et al., 2016). PGRN is also an anti-inflammatory molecule that directly binds to TNFR, inhibits TNFα/TNFR1 inflammatory signaling (Liu and Bosch, 2012; Jian et al., 2013b; Liu, 2011; Tian et al., 2014;

* Corresponding author at: Rm 1608, Department of Orthopedic Surgery, New York University Medical Center, 301 East 17th Street, New York, NY 10003, USA.
E-mail address: chuanju.liu@med.nyu.edu (C. Liu).
[1] Current address: National Centre for Inherited Metabolic Disorders. Department of Medicine, Mater Misericordiae University Hospital and University College Dublin, Ireland.

https://doi.org/10.1016/j.ebiom.2018.01.022

Tian et al., 2012; Zhao et al., 2013a; Tang et al., 2011), and activates the TNFR2 anti-inflammatory pathway (Zhao et al., 2015; Zhao et al., 2013b; Wei et al., 2014b; Li et al., 2014; Fu et al., 2017). Autoantibodies against PGRN have been detected in sera from patients with colitis, rheumatoid arthritis, and other autoimmune diseases, and these antibodies block PGRN binding to TNFR (Thurner et al., 2013a; Thurner et al., 2015; Thurner et al., 2014; Thurner et al., 2013b). Insufficiency of PGRN also associates with various types of CNS diseases, including frontotemporal lobe dementia (haploinsufficiency) (Baker et al., 2006; Cruts et al., 2006), Alzheimer disease (Brouwers et al., 2008), and Parkinson disease (Hu et al., 2006; Brouwers et al., 2007). In addition, intracellular PGRN plays an important role in lysosome biology, and homozygous deficiency of PGRN causes lysosomal storage diseases, including neuronal ceroid lipofuscinosis (Ahmed et al., 2010; Smith et al., 2012) and Gaucher-like disease (Jian et al., 2016a; Choy and Christensen, 2016; Jian et al., 2016b). Serum levels of PGRN are significantly decreased in GD patients, and *GRN* variants were found to be prevalent in GD patients. PGRN-deficient mice develop a typical GD-like phenotype. Mechanistically, PGRN functions as a chaperone that facilitates the lysosomal delivery of GCase, the defective enzyme in GD (Jian et al., 2016a; Jian et al., 2016b). This function of PGRN may be operative with other lysosome enzymes (Jian et al., 2017). Interestingly, PGRN and a PGRN-derived peptide, Pcgin, ameliorated GD phenotypes in mouse models and fibroblasts obtained from GD patients.

Chitinases (EC 3.2.2.14) are hydrolytic enzymes that break down glycosidic bonds in chitin (Rathore and Gupta, 2015). They belong to 18 glycosyl hydrolase family, an ancient gene family that is widely expressed from prokaryotes to eukaryotes. Chitotriosidase (CHIT1) was the first discovered and characterized mammalian chitinase (Boot et al., 1998). CHIT1 has been used as a biomarker for lysosomal storage diseases, including GD (Hollak et al., 1994; Wajner et al., 2004; van Dussen et al., 2014) and Niemann Pick diseases (Wajner et al., 2004). CHIT1 protein and enzymatic activity levels decrease with enzyme replacement therapy in GD patients (Drugan et al., 2017). Chitinase-3-like protein 1 (CHI3L1), also called YLK-40 (based on its three N-terminal amino acids: tyrosine (Y), lysine (K), and leucine (L)), is a 40 kDa mammalian glycoprotein. CHI3L1 binds chitin polymers but lacks chitinase activity. CHI3L1 is a pro-inflammatory marker and elevations of CHI3L1 have been found in auto-immune diseases, such as rheumatoid arthritis, pulmonary sarcoidosis (Di Rosa et al., 2016), psoriasis (Baran et al., 2017), interstitial lung disease (Hozumi et al., 2017), hypertension (Xu et al., 2017), and various types of cancer (Erturk et al., 2017; Kotowicz et al., 2017; Shaker and Helmy, 2017; Wan et al., 2017). CHI3L1 binds to IL-13 receptor α2, and exerts its biological function by activating downstream mitogen-activated protein kinase, protein kinase B/AKT, and Wnt/β-catenin signaling (He et al., 2013). In this study CHI3L1 was identified as a novel downstream molecule that has potential to be employed as a novel biomarker for diagnosing GD and for examining the therapeutic effects of new GD drug(s).

2. Material and Methods

2.1. Reagents

Fibroblasts from GD patients with L444P homozygosity were purchased from Coriell Cell Repositories (Camden, NJ) and cells were cultured in DMEM supplemented with 10% FBS. Antibodies against CHI3L1 and GAPDH were purchased from Santa Cruz Biotechnology (Dallas, Texas).

2.2. Gene Expression Analysis

C57BL/6 WT mice and PGRN KO mice were maintained at NYU Animal Facility in accordance with an Institutional Animal Care and Use Committee approved protocol. Comparative gene array analysis between WT and PGRN KO CD4+ T cells has been described previously (Mundra et al., 2016). Briefly, naïve $CD4^+$ T cells were isolated from spleen of WT and PGRN KO mice, and activated using CD3 and CD28 antibody (Ab) over 24 h. RNA was extracted and quantified with NanoDrop ND-1000. RNA integrity was assessed by standard denaturing agarose gel electrophoresis. The Mouse 4 × 44K Gene Expression Array v2 (Agilent Technology) with about 39,000+ mouse genes and transcripts represented, all with public domain annotations, was employed for genomic profiling. Sample labeling and array hybridization were performed according to the Agilent One-Color Microarray-Based Gene Expression Analysis protocol (Agilent Technology). Agilent Feature Extraction software (version 11.0.1.1) was used to analyze the acquired array images. Quantile normalization and subsequent data processing were performed with using the GeneSpring GX v11.5.1 software (Agilent Technologies). Differentially expressed genes were identified through Fold Change filtering.

2.3. Real-time Quantitative PCR

Various tissues, including spleen and lung, from WT and PGRN KO mice were dissected and homogenized in TRIzol® reagent. RNA extraction was performed in accordance with the manufacturer's recommended protocol. cDNA was synthesized using SuperScript® Reverse Transcriptase (Invitrogen). SYBR® Green PCR Master Mix (Applied Biosystems) was employed in real-time PCR and the reaction was performed with StepOnePlus™ Real-Time PCR Systems (Applied Biosystems). The mRNA levels of target genes were normalized to GAPDH. The following sequence-specific primers were used for the real-time qPCR: 5′- ACGATTTCCATGGA GTCTGG-3′ and 5′- AATCCTTCCCCTGAGATTGG -3′ for mouse CHI3L1, 5′-CCAGCATATG GGCATACCTT-3′ and 5′-CAGACCTCAGTGGCTCCTTC -3′ for mouse CHI3L3, 5′-CAGTGG CTCAAGGACAACAA-3′, 5′-CGTGGAAAAACCGTTGAAGT-3′ mouse CHI3L4. The presence of a single specific PCR product was verified by melting curve analysis and the experiments were repeated three times.

2.4. GD Mouse Model

The induction of the GD phenotype in PGRN null mice has been described (Jian et al., 2016a; Jian et al., 2016b). Briefly, the GD phenotype was induced in 8 week-old C57B/L6 WT and PGRN KO mice by (intraperitoneal) IP injection of OVA-Alum (Aluminium hydroxide-emulsified Ovalbumin) at Day 1 and Day 15, followed by intranasal challenge of 1% OVA beginning at Day 29 at a frequency of three times per week for four weeks. In rescue experiments, 4 mg/kg recombinant PGRN or Pcgin, or 60 U/kg imiglucerase were IP injected weekly following initiation of intranasal challenge. Spleens, livers, limbs, and lungs were collected at sacrifice.

D409V/- GD mouse is a model generated by disruption of one *Gba1* allele, and point mutation, D409V, on the other allele (Barnes et al., 2014). The D409V GCase is unstable and rapidly degraded (Liou et al., 2006) and the D409V/- mice develop Gaucher cells at around 8 weeks of age. At 5-weeks-old, D409V/- mice were injected with rPGRN (4 mg/kg/week) for 4 weeks and then sacrificed for examination of CHI3L1 expression from spleen lysate ($n = 6$ per group).

2.5. Isolation of Organelle From Spleen Tissues

Spleens from WT and PGRN KO mice with OVA challenge were dissected and the cellular organelles were isolated by using a modified protocol of the Lysosome Isolation Kit (Sigma-Aldrich). Briefly, spleen tissues were homogenized in 1 mL 1× Extraction buffer (provided by the kit) and centrifuged at 1,000 ×*g* for 10 min at 4 °C. The upper lipid layer was removed and the supernatant was transferred to a sterile Eppendorf tube. Another 1 mL Extraction buffer was added to the pellet and the homogenization was repeated. Pellets containing nuclei and cellular debris were discarded and supernatant was centrifuged at

20,000 ×*g* for 20 min at 4 °C. Pellets containing mitochondria, lysosomes, peroxisomes and endoplasmic reticulum were suspended in SDS-loading buffer and submitted for Mass Spectrometry analysis.

2.6. Mass Spectrometry Analysis

Mass Spectrometry analysis was performed at the proteomic core facility at New York University School of Medicine as described (Jian et al., 2016a). Briefly, protein samples were reduced with DTT at 57 °C for 1 h and alkylated with iodoacetamide at RT in the dark for 45 min. Samples were loaded onto a NuPAGE® 4–12% Bis-Tris Gel 1.0 mm and stained with GelCode Blue Stain Reagent (Thermo Scientific). Excised gel pieces were de-stained and dehydrated with an acetonitrile rinse and further dried in a SpeedVac concentrator for 20 min. Proteins were digested overnight with sequencing grade-modified trypsin (Promega). High resolution full MS spectra were acquired with a resolution of 70,000, an AGC target of 1e6, with a maximum ion time of 120 ms, and the scan range of 300 to 1500 *m/z*. Following each full MS twenty data-dependent high resolution HCD MS/MS spectra were acquired. All MS/MS spectra were collected using the following instrument parameters: resolution of 17,000, AGC target of 2e5, maximum ion time of 250 ms, one microscan, 2 m/z isolation window, fixed first mass of 150 m/z, and NCE of 27. MS/MS spectra were searched against a Uniport mouse database using Sequest within Proteome Discoverer.

2.7. SDS-PAGE and Western Blotting

Protein samples from lyses of WT and PGRN null mouse tissues were separated by SDS-PAGE and transferred to a nylon membrane after electrophoresis. The membrane was probed with the primary antibody overnight at 4 °C and incubated with secondary antibody for 2 h at room temperature. The bands were developed on the film using ECL Prime Western Blotting Detection Reagent (Amersham Pittsburgh, PA).

2.8. Immunohistochemistry

Paraffin-embedded lung sections from WT and PGRN KO mice were de-paraffinized with xylene and hydrated via ethanol gradient. Antigen was retrieved by using 0.1% trypsin in 0.1% CaCl2 at 37 °C for 30 min. Endogenous hydrogen peroxidase was inactivated by incubation with 3% H_2O_2 in PBS for 10 min. The slides were blocked with 3% BSA and 20% goat serum for 30 min. Primary antibodies were diluted at 1:20–50 with 2% goat serum and primed on the slides at 4 °C overnight. The next day, slides were washed with PBS and secondary antibody was added (1:200 biotin-labeled goat-anti rabbit antibody or goat-anti mouse antibody) for 1 h. The staining was visualized by Vector ABC peroxidase kit, followed by DAB substrate.

2.9. ELISA Quantification of CHIT1 and CHI31L From Human Sera

Sera from 115 GD patients with N370S mutation in *GBA1*, and 55 healthy controls from Ashkenazi Jews were collected from New York University Medical Center and Mount Beth Israel Medical Center, as reported previously (Jian et al., 2016b). Serum PGRN level was measured as previously described (Jian et al., 2016b). Serum levels of CHIT1 and CHI3L1 were quantified using kits from Aviva Systems Biology (San Diego, CA). Briefly, the ELISA plates were blocked with 300 μl blocking buffer for 30 min. After blocking, buffer was discarded and 100ul of sera, diluted ten-fold in sterile PBS, and appropriate standards were loaded and incubated for 2 h. Plates were washed with PBS 5 times and 100 μl Detection Antibody was added for 1 h. Plates were washed again and 100 μl Detector was added for 1 h. Plates were rinsed and 100 μl TMB Substrate Solution was added and the reaction was terminated by Stop solution. The results were readout at 450 nm using a plate reader. The concentrations of CHIT1 and CHI31L were calculated based on the standard curve.

2.10. Statistical Analyses

Student *t*-tests were used to compare serum levels of PGRN, CHI3L1 and CHIT1 in healthy controls and GD patients. The correlations of PGRN, CHI3L1, and CHIT1 were plotted by linear correlation and the statistical significance were analyzed by Pearson correlation method. For comparison of treatment groups, we performed unpaired t-tests, paired t-tests, and one-way or two-way ANOVA (where appropriate). All statistical analysis was performed using SPSS Software. Statistical significance was two-sided and was achieved when at $p < 0.05$.

3. Results

3.1. Chitinase-3 Like Family Members Were Up-regulated in PGRN Null Mice

Previously, we have found that PGRN directly binds to TNFR and is therapeutic against inflammatory arthritis (Tang et al., 2011). In addition to antagonizing TNFα activity, PGRN potently stimulates T_{reg} population and enhances production of anti-inflammatory cytokine IL-10 (Fu et al., 2016; Wei et al., 2014a). To investigate the molecular mechanisms of PGRN in T cell function, naïve $CD4^+$ T cells from WT and PGRN null mice were isolated and activated by CD3 and CD28 antibody treatment. Total RNA was extracted for gene array analysis, as reported previously (Mundra et al., 2016). Approximately 2600 genes were differentially regulated in PGRN null mice as compared to WT mice and about 1200 of these were up-regulated (Mundra et al., 2016). Of these up-regulated genes 350 genes were increased >4.5-fold. Chemokine family members, CXCL9 and CXCL10, were dramatically induced (Mundra et al., 2016). Also, Chitinase-3 like family mRNAs were significantly induced in PGRN null $CD4^+$ T cells (Fig. 1A, B); specifically, Chitinase-3-like-3 (CHI3L3) was increased 21.3 fold, Chitinase-3-like 4 (CHI3L4) was increased 8.2 fold, and Chitinase-3-like-1 (CHI3L1) was increased 4.9 fold (Fig. 1A, B).

To confirm the gene array data and to examine the expressions of Chitase-3 like family members in other tissues, RNA from liver, spleen, kidney, lung, and brain from WT and PGRN KO mice, were assessed quantitatively by real-time PCR for expression of CHI3L1, CHI3L3, and CHI3L4. CHI3L1 mRNA increased ~8-fold in spleen of PGRN null vs WT, while in other tissues the level of CHI3L1 was comparable to WT (Fig. 1B). The CHI3L3 mRNA levels varied between tissues with reduced levels in liver, kidney, and lung of PGRN null mice, but comparable in spleen and slightly increased in brain relative to WT (Fig. 1B). CHI3L4 was undetectable in liver from PGRN null and WT mice, whereas its levels were increased ~10-fold in spleen, and 7-fold in kidney of PGRN null mice. CHI3L4 mRNA had comparable levels in WT and PGRN null in lungs and brains (Fig. 1B). The gene array and qPCR demonstrated that Chitinase-3 like family members, especially CHI3L1 and CHI3L4, were induced in spleen of PGRN null mice.

3.2. CHI3L1 is Enriched in the Organelles in PGRN Null Mice With GD-like Phenotypes

In a previous effort to determine the role of PGRN in lung inflammation, we challenged PGRN null mice with Ovalbumin (OVA) and found that PGRN KO mice developed prominent GD-like phenotypes unexpectedly. The OVA-induced inflammation is a stressor that accelerates the development of GD-like phenotypes in adult PGRN KO mice, while aged PGRN KO mice develop GD-like phenotypes spontaneously (Jian et al., 2016a; Jian et al., 2016b). Intracellular PGRN was shown to be essential for GCase trafficking to the lysosome (Jian et al., 2016a; Jian et al., 2016b). PGRN does not affect GCase protein expression and enzymatic activity in total cell extracts, but is required for delivery of GCase to lysosomes in a HSP70 dependent manner (Jian et al., 2017). Without PGRN, GCase becomes aggregated in cytoplasm, especially under stress conditions (Jian et al., 2016b). To find other proteins that may be affected by the absence of PGRN, MS analyses of enriched organelles,

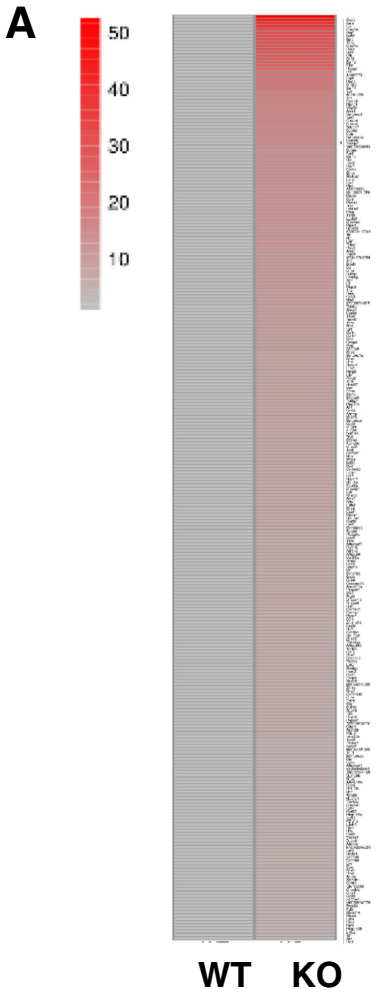

GeneSymbol	Absolute Fold change ([KO] vs [WT])	GenbankAccession
CXCL9	69.64398	NM_008599
IL17A	30.417433	NM_010552
CLEC4N	29.998985	NM_020001
PROCR/EPCR	29.386135	NM_011171
CHI3L3	21.319992	NM_009892
CXCL10	18.357534	NM_021274
IL1B	18.21715	NM_008361
CCL6	13.378497	NM_009139
IL9	12.657534	NM_008373
IL15	11.696849	NM_008357
CCL17	9.807823	NM_011332
CHI3L4	8.241861	NM_145126
CCL9	6.3938775	NM_011338
ZMYND15	6.391433	NM_001029929
CHI3L1	4.85125	NM_007695
IL21	4.602642	NM_021782
IL13	4.4472957	NM_008355
CXCR5	4.3540134	NM_007551
CCR5	3.483887	NM_009917
CXCR3	3.4829118	NM_009910

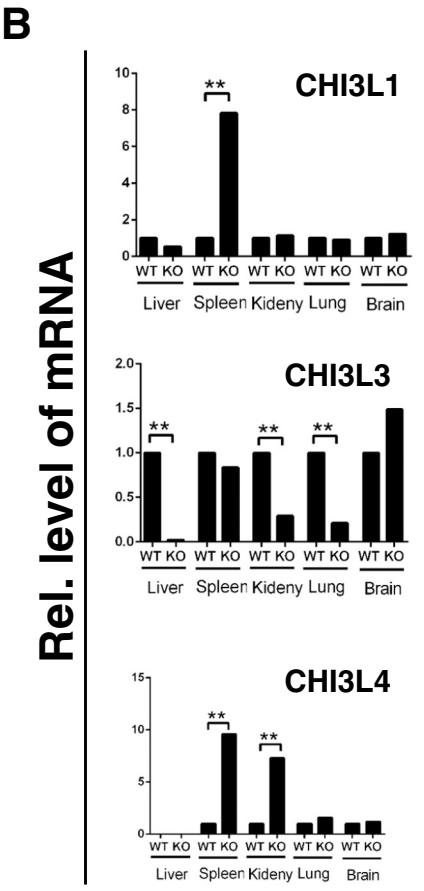

Fig. 1. Chitase-3 like family members were increased in PGRN KO mice. (A) Gene array analysis of gene expression profile of $CD4^+$ T cells from WT and PGRN KO mice. Naive $CD4^+$ T cells were isolated from spleen of WT and PGRN KO mice, and activated overnight with CD3 and CD28 antibodies. The mRNA was isolated and analyzed using the Mouse Gene Expression Array v2 (Agilent Technology). Genes upregulated >4.5 fold were shown. The fold change of Chitase-3 like family members and other cytokines is indicated in Table. (B) Expression of Chitase-3 like family members in various tissues. Liver, spleen, kidney, lung, and brain were dissected from WT and PGRN KO mice. RNA was extracted and expressions of Chitase-3 like family members were determined by quantitative real-time PCR. The expressions were normalized with housekeeping gene GAPDH. Figure is representative of three independent experiments.

including lysosome, endoplasmic reticulum and mitochondria from splenic extracts from two WT and two PGRN null mice were conducted after induction of the GD phenotype (Fig. 2A). Average of (Peptide Spectrum Matches PSM) of each hit was calculated from two WT and two PGRN null mice, respectively. The ratio of average PSM in PGRN null to average PSM in WT mice was calculated, and hits that increased or decreased >2-fold were sorted (Fig. 2B). Seven proteins were identified that had increased in PGRN null organelles, and 23 proteins were decreased in PGRN null organelles. Among the 7 proteins, we found CHI3L1, with highest PSM score, was 2.43-fold higher in PGRN null organelles than it in WT organelles (Fig. 2B).

3.3. The Expression of CHI3L1 is Elevated in PGRN Null GD Animal Model

Using two independent non-biased screens targeting the RNA and protein levels respectively, CHI3L1 levels were increased in PGRN null mice, especially after induction of GD phenotype. To confirm the gene array and mass spectrum data, splenic lysates were prepared from WT and PGRN null mice, with or without OVA challenge using 5 mice in each cohort. By western-blot analyses, CHI3L1 was increased following OVA challenge in WT mice, and it was higher in PGRN null mice, both at resting level and after OVA challenge, in particular the latter (Fig. 3A–B). Given that lung tissue from PGRN null mice showed a typical GD-like phenotype and was full of Gaucher cells (Jian et al., 2016b; Jian et al., 2016a), the expression of CHI3L1 in lung tissues was also examined using immunohistochemistry. Interestingly, although CHI3L1 mRNA level remained unchanged in the lungs of PGRN null mice (Fig. 1B), markedly strong staining of CHI3L1 was observed in typical "giant" Gaucher cells of PGRN null mice after OVA challenge when compared to WT after OVA challenge (Fig. 3C), suggesting that the elevated CHI3L1 protein level seen in PGRN null GD model may result from altered post-transcriptional regulation, such as increased RNA stability and/or reduced protein degradation.

In a separate effort to analyze the developmental global gene expressions in GD, lung tissues from age-matched WT and *Gba1* D409V/null mice at different ages (4 w, 8 w, 18 w, 28 w) were collected for microarray analysis (Xu et al., 2011). Intriguingly, CHI3L1 expression increased around 5-fold in *Gba1* D409V/null macrophages vs WT at 4 weeks-old, and its levels reached a relative increase of ~10-fold in 8-week–old mice. Following the 8 week timepoint, the CHI3L1 level reduced gradually and became a 2-fold increase in adult *Gba1* D409V/null mice (28 week-old) vs WT mice (Fig. 3D),

3.4. CHI3L1 Expression is Reduced Following Treatment of GD in Animal Models

Since PGRN null mice develop a GD phenotype after OVA challenge (Jian et al., 2016b) and CHI3L1 is significantly increased in this GD

A

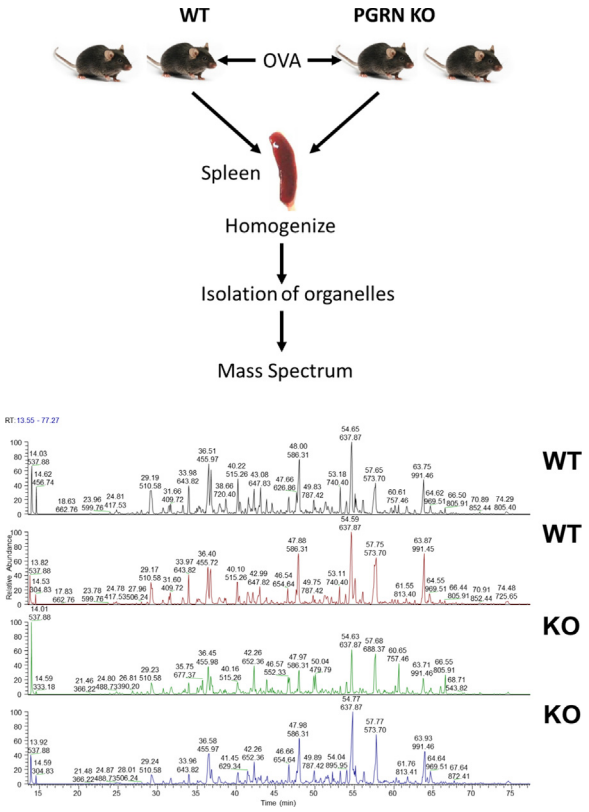

B

Gene name	Average KO	Average WT	RATIO
Myosin-14	111	37.5	2.96
Myosin-10	56	19.5	2.85
Myosin-11	50	19	2.63
Plec	43	16.5	2.58
Chitinase 3 like 1	211	87	2.43
Aldh6a1	23	11	2.05
Letm1	16	8	2.00
Apolipoprotein A-I	23	46	0.50
Tropomyosin	10	20.5	0.49
Eosinophil peroxidase	10	20	0.48
lipocalin	5	9.5	0.47
Tropomyosin	11	22.5	0.47
Dematin	6	13	0.46
Basigin	6	12	0.46
Ankyrin-1	67	146	0.46
Antithrombin-III	7	15.5	0.45
Epb42	20	45	0.43
Glycophorin A	9	21	0.43
anion transport protein	54	126.5	0.42
Tropomyosin 1	9	20.5	0.41
Tropomyosin	4	8.5	0.41
adducin 1	7	17.5	0.40
Stom	8	20	0.38
Mpp1	17	44.5	0.37
Pyruvate kinase	6	17.5	0.34
Myosin-6	4	13	0.31
Epb42	11	36	0.29
Alpha-1-antitrypsin	16	55.5	0.29
Ubiquitinyl hydrolase 1	2	7	0.29
Adducin 2	2	12.5	0.16

Fig. 2. CHI3L1 was enriched in organelles in PGRN KO mice after OVA challenge. (A) Illustration of method to identify proteins changed in organelles in PGRN KO mice. Briefly, two WT and two PGRN KO mice were challenged with OVA, and spleens were dissected for isolating organelles. The enriched organelles were analyzed by Mass Spectrometry at NYU Core facility. (B) Genes enriched or reduced significantly in PGRN KO organelles. The average PSM of WT is ratio with average PSM of PGRN KO mice, changes increased or decreased more than two-fold were listed as significantly.

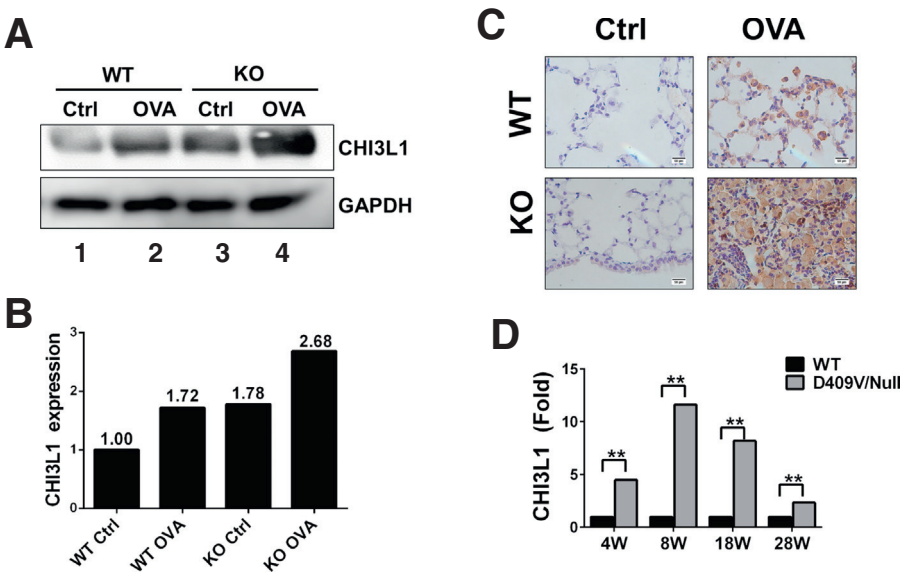

Fig. 3. CHI3L1 expression was increased in PGRN KO GD animal model. WT and PGRN KO mice received IP injection of OVA at Day 1 and 15, followed by intranasal challenge of 1% OVA at Day 29 for three times per week for four weeks. Spleen tissues were lysed and the level of CHI3L1 was measured by Western blotting (A) and quantified by Image J (B) and the sections of lung tissues were analyzed by immunohistochemistical staining (C). Lungs were collected from aged-matched WT and *Gba1* D409V/-mice at 4w, 8w, 18w and 28w. RNA were extracted and hybridized with microarray chip as previously reported (Xu et al., 2011), CHI3L1 expression increased in *Gba1* D409V/-mice (D).

animal model, we tested whether expression of CHIT3L1 correlated with GD progression. Mice with GD phenotype following OVA challenge and a second group of mice were given injection of Imiglucerase (60 U/kg/week, for four weeks, serving as a positive control). Imiglucerase, modified recombinant GCase used to treat human GD, significantly reduced GD histology, including reduced Gaucher cell number and size (Jian et al., 2016b). Concomitantly, the CHI3L1 level was reduced by imiglucerase treatment (Fig. 4A).

As recombinant PGRN and Pcgin ameliorated GD-like phenotypes in multiple models (Jian et al., 2016a; Jian et al., 2016b), PGRN and Pcgin were examined for effects on CHI3L1 expression. PGRN null mice OVA-induced GD phenotype was used. One group of these PGRN null mice received PGRN protein (4 mg/kg/week), and another group mice received Pcgin (4 mg/kg/week). CHI3L1 levels were increased concomitant with the development of the GD phenotype and were found to be significantly reduced in both PGRN- and Pcgin-treated groups as assayed by Western blotting (Fig. 4B, C) and by immunohistochemical staining (Fig. 4D). In addition to our PGRN KO GD animal model, we also tested whether PGRN reduced CHI3L1 expression in D409V/-mice. D409V/- develop a GD phenotype spontaneously around 8 weeks of age (Barnes et al., 2014). Recombinant PGRN protein also markedly reduced CHI3L1 expression in spleen tissues of the *Gba1* mutated D409V/null animal model (Fig. 4E–F).

3.5. CHI3L1 Expression is Reduced Followed Treatment of PGRN and Pcgin in GD Fibroblasts

CHI3L1 levels were increased in PGRN null GD animal models, and declined following treatment with imiglucerase, PGRN, or Pcgin (Fig. 4). Next, CHI3L1 expression was assessed in GD patient fibroblasts following treatment with imigluerase, PGRN, or Pcgin. Fibroblasts from GD patients with L444P homozygosity were treated with PGRN (1 μg/ml), Pcgin (1 μg/ml), or Imiglucerase (160 mU/ml) for 24 and 48 h respectively. After 24 h treatment, cells were collected for mRNA analysis. As shown in Fig. 4G, CHI3L1 mRNA was significantly reduced following treatment with PGRN, Pcgin or Imiglucerase. After 48 h of treatment, cells were collected to compare the CHI3L1 expression at protein level. Similar to the changes at mRNA level, CHI3L1 protein level was also reduced by PGRN, Pcgin, or imiglucerase treatment (Fig. 4H, I).

3.6. Serum Level of CHI3L1 is Increased in GD Patients

The findings that increased CHI3L1 expression is associated with PGRN insufficiency and development of a GD-like phenotype and CHI3L1 level is responsive to treatment with FDA-approved drug imiglucerase or with recombinant PGRN or PGRN-derived Pcgin, together with the fact that CHI3L1 belongs to the same chitinase family, as established GD biomarker CHIT1 (Giraldo et al., 2001), prompted us to determine whether CHI3L1 can also be employed as a new biomarker for GD patients.

Serum levels of CHIT1, CHI3L1 and PGRN were measured from 121 GD patients and 55 healthy controls of Ashkenazi Jewish descent by ELISA. In line with previous reports, the levels of CHIT1 were significantly higher in GD patients than healthy controls (35.07 ± 2.099 ng/ml in control vs 51.16 ± 2.824 ng/ml in GD, 95% CI: 7.551 to 24.62, $p < 0.001$) (Fig. 5A). The level of CHI3L1, similar to CHIT1, was increased in GD patients compared with healthy controls (684.7 ± 68.20 pg/ml in control vs 1736 ± 152.1 pg/ml in GD, 95% CI: 604.9 to 1498, $p < 0.001$) (Fig. 5B). Conversely, the PGRN level was reduced in GD patients, from 150.6 ± 4.501 ng/ml in control to 91.56 ± 3.986 ng/ml in GD, 95 CI: −72.10 to −46.05, $p < 0.001$ (Fig. 5C).

Analysis of correlations among PGRN, CHI3L1, and CHIT1 in both healthy controls and GD patients, surprisingly revealed that CHI3L1 and PGRN were positively correlated in both healthy controls and GD patients; albeit the correlation in healthy controls ($r = 0.3261$, $P = 0.0237$) was weaker than in GD patients ($r = 0.357$, $p < 0.001$) (Fig. 6A–C). Interestingly, there was no correlation between CHIT1 and PGRN in healthy controls ($r = 0.223$, $p = 0.1014$); however, a strong positive correlation was found in GD patients ($r = 0.44075$, $p < 0.001$) (Fig. 6D–F). Similarly, there was no correlation between CHI3L1 and CHIT1 in healthy controls ($r = 0.1517$, $p = 0.3031$), while a significant positive correlation was found in GD patients ($r = 0.2081$, $p = 0.025$) (Fig. 6G–I). These results clearly indicate PGRN, CHI3L1 and CHIT1 are functionally closely related, especially in GD patients.

4. Discussion

CHI3L1 is a secreted glycoprotein produced by a variety of cells, including neutrophils, monocytes/macrophages, osteoclasts and other

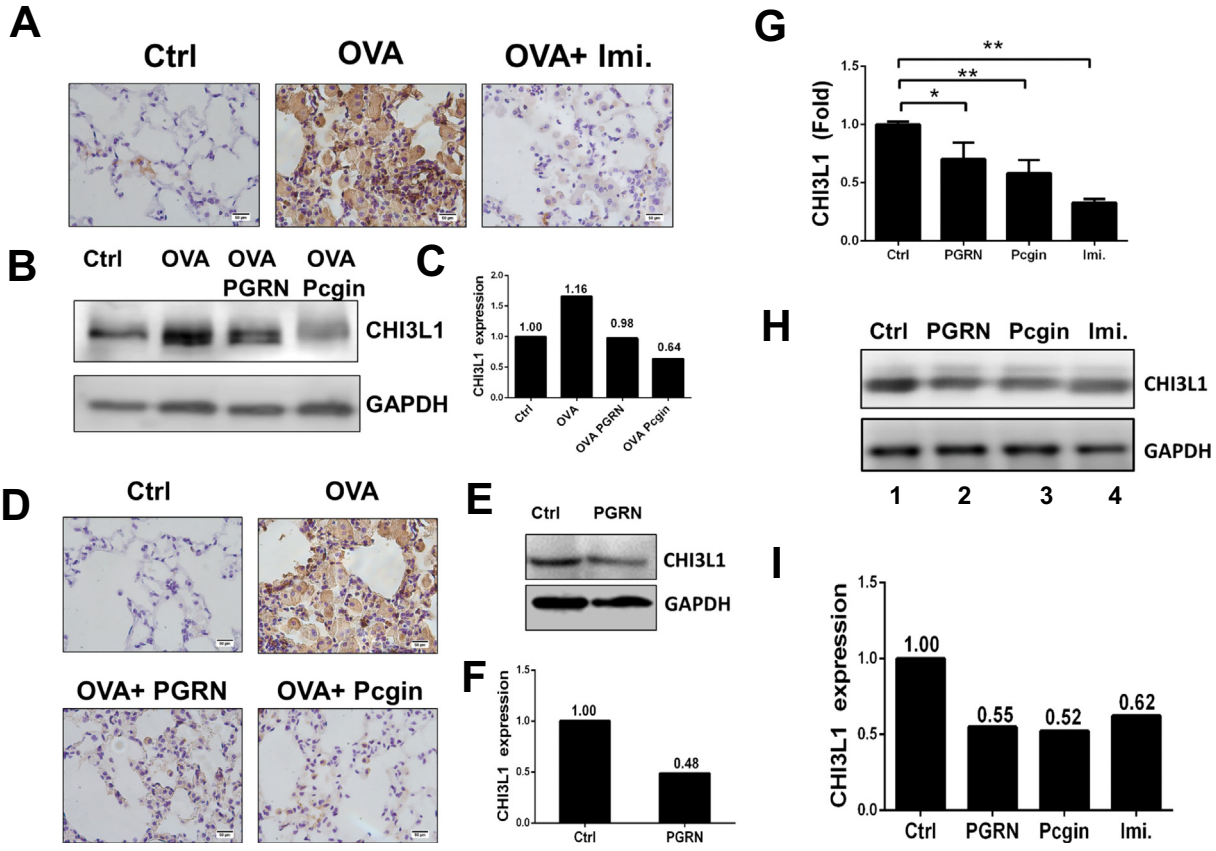

Fig. 4. CHI3L1 level was reduced following treatment of GD. (A) Imiglucerase treatment led to reduced level of CHI3L1 in the PGRN KO GD animal model. PGRN KO mice were induced toward a GD phenotype by IP injection of OVA at Day 1 and 15, followed by intranasal challenge of 1% OVA at Day 29 for three times per week for four weeks. One group of mice received imiglucerase (60 μg/kg/week) after Day 29 for four weeks. Lung tissues were collected for immunohistochemistry staining with CHI3L1 specific antibody. (B) PGRN KO mice were induced toward a GD phenotype. Two groups of PGRN KO mice received IP injection of recombinant PGRN protein (4 mg/kg/week) and Pcgin (4 mg/kg/week), respectively, starting after Day 29 for four weeks. Spleen tissues were collected to analyze CHI3L1 expression by western-blot. (C) Quantification of (B) using Image J. (D) Lung tissue sections from PGRN KO mice treated with PGRN or Pcgin from (B) were stained with CHI3L1 specific antibody. (E) Recombinant PGRN injection reduced CHI3L1 expression in *Gba1* D409V/null GD mouse model. 5-weeks-old D409V/null mice were injected with PBS or rPGRN (4 mg/kg/week) for 4 weeks and CHI3L1 expression was measured in spleen lysis. (F) Quantification of (E) by Image J. (G–I) CHI3L1 expressions at both mRNA level (G) and protein level (H) were reduced in the fibroblasts of GD patients following treatment with imiglucerase, PGRN, or Pcgin. Fibroblasts were treated with imiglucerase (160 mU/ml), PGRN (1 μg/ml), and Pcgin (1 μg/ml) for 24 and 48 h respectively. The CHI3L1 mRNA levels were measured by quantitative PCR after 24 h and protein levels were examined by western-blot after 48 h treatment. (I) Quantification of (H) by Image J.

tissues (Di Rosa et al., 2014). CHI3L1 is able to bind to Chitin, but lacks enzymatic activity to cleave Chitin. CHI3L1 is considered a pro-inflammatory marker, as it stimulates production of inflammatory mediators (e.g., CCL2, CXCL2, MMP-9) (Libreros et al., 2012), and has been reported to be associated with various kinds of autoimmune disorders, including colitis, rheumatoid arthritis, systemic sclerosis, diabetic mellitus, and asthma (Di Rosa et al., 2016). CHI3L1 is considered a cancer marker as well, since its expression is associated with various types of cancer, including melanoma (Erturk et al., 2017), thyroid carcinoma (Luo et al., 2017), colorectal cancer (Shantha Kumara et al., 2016), and breast cancer (Chen et al., 2017). Although CHI3L1 has multiple biological functions, the molecular mechanisms by which CHI3L1 is involved in a wide spectrum of diseases are still unclear. Notably, CHI3L1 is a key molecule in the regulation of macrophage function, and CHI3L1 has been

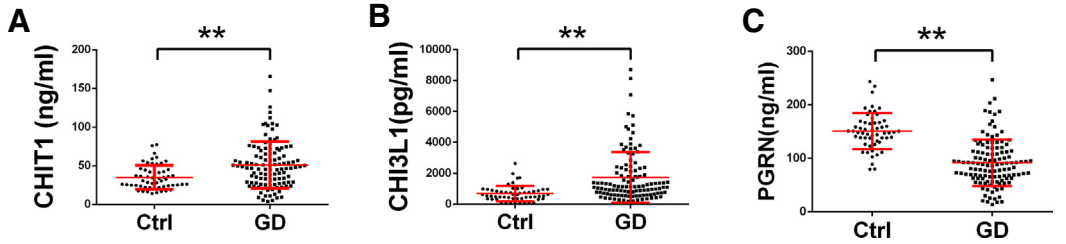

Mean ± SEM of Ctrl	35.07 ± 2.099
Mean ± SEM of GD	51.16 ± 2.824
Difference between means	16.09 ± 4.323
95% CI	7.551 to 24.62
R square	0.07657

Mean ± SEM of Ctrl	684.7 ± 68.20
Mean ± SEM of GD	1736 ± 152.1
Difference between means	1051 ± 226.2
95% confidence interval	604.9 to 1498
R square	0.1134

Mean ± SEM of column A	150.6 ± 4.501
Mean ± SEM of column B	91.56 ± 3.986
Difference between means	-59.08 ± 6.599
95% confidence interval	-72.10 to -46.05
R square	0.3153

Fig. 5. Serum levels of CHIT1, CHI3L1 and PGRN. Sera from 121 GD patients and 55 healthy controls from Ashknaiz Jewish descent were used to measure CHIT1, CHI3L1 and PGRN level by ELISA kits. Student's *t*-test was used to compare the levels of those molecules in healthy controls and GD patients (** stands for $p < 0.01$).

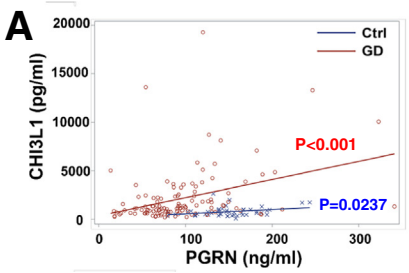

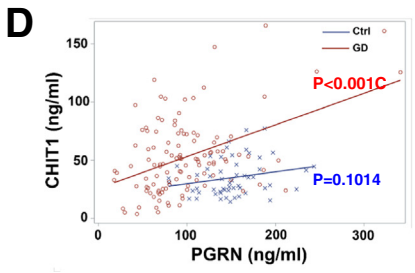

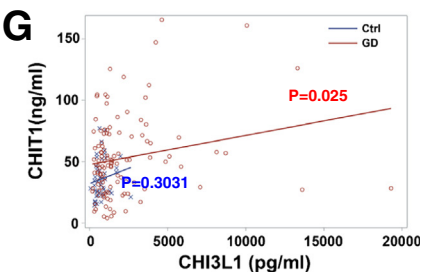

B Correlation PGRN and CHI3L1 in healthy control

Variable	N	Mean	Std Dev	Sum	Min.	Max.
CHI3L1	48	774.8	478.4	37189	69.2	2635
PGRN	55	150.6	33.9	8285	79.3	243.4

Pearson correlation Coefficiency

	CHI3L1	PGRN
CHI3L1	1.000	0.3261 0.0237
PGRN	0. 0.3261 0.0237	1.000

E Correlation PGRN and CHIT1 in healthy control

Variable	N	Mean	Std Dev	Sum	Min.	Max.
PGRN	55	150.6	33.9	8285	79.3	243.4
CHIT1	55	35.1	15.6	1929	14.3	77.2

Pearson correlation Coefficiency,

	PGRN	CHIT1
PGRN	1.000	0.223 0.1014
CHIT1	0.223 0.1014	1.000

H Correlation CHI3L1 and CHIT1 in healthy control

Variable	N	Mean	Std Dev	Sum	Min.	Max.
CHI3L1	48	774.8	478.4	37189	69.2	2635
CHIT1	55	35.1	15.6	1929	14.3	77.2

Pearson correlation Coefficiency

	CHI3L1	CHIT1
CHI3L1	1.000	0.15176 0.3031
CHIT1	0.15176 0.3031	1.000

C Correlation PGRN and CHI3L1 in GD paitents

Variable	N	Mean	Std Dev	Sum	Min.	Max.
CHI3L1	121	2140	2801	258990	187.95	19292
PGRN	116	95.5	53.3	11556	13.7	341.1

Pearson correlation Coefficiency

	CHI3L1	PGRN
CHI3L1	1.000	0.357 <0.001
PGRN	0.357 <0.001	1.000

F Correlation PGRN and CHIT1 in GD patients

Variable	N	Mean	Std Dev	Sum	Min.	Max.
PGRN	121	95.5	53.2	11556	13.7	341.1
CHIT1	116	52.7	32.3	6118	3.84	165.6

Pearson correlation Coefficiency

	PGRN	CHIT1
PGRN	1.000	0.44075 <0.001
CHIT1	0.44075 <0.001	1.000

I Correlation CHI3L1 and CHIT1 in GD patients

Variable	N	Mean	Std Dev	Sum	Min.	Max.
CHI3L1	121	2140	2801	258990	187.95	19292
CHIT1	116	52.7	32.3	6118	3.84	165.6

Pearson correlation Coefficiency

	CHI3L1	CHIT1
CHI3L1	1.000	0.20807 0.025
CHIT1	0.20807 0.025	1.000

Fig. 6. Correlation analysis of CHI3L1, PGRN and CHIT1. Serum levels of CHI3L1, PGRN, and CHIT1 were plotted with each other individually by SPSS software, and Pearson correlation were analyzed in healthy controls and GD patients respectively ($p < 0.05$ is statistical significance) A–C: Correlation between PGRN and CHI3L1; D–F: Correlation between PGRN and CHIT1; and G–I: Correlation between CHIT1 and CHI3L1.

implicated in above diseases, at least partially through its regulation of macrophages (Letuve et al., 2008; Junker et al., 2005; Kumagai et al., 2016).

GD is characterized by accumulation of lipid-engorged macrophages, resulting from GlcCer accumulation as a consequence of reduced enzymatic activity of GCase (Futerman and Platt, 2017; Grabowski, 2017). A recent study demonstrated that the immune system, in particular complement C5, also plays an important role in the pathogenesis of GD (Pandey et al., 2017). PGRN is a newly identified regulator of GD through direct binding to GCase and facilitating the delivery of GCase to lysosome (Jian et al., 2016b). Deficiency of PGRN led to typical GD phenotypes in mice (Jian et al., 2016b). In addition, *GRN* gene mutations are widely present in GD patients and serum levels of PGRN are significantly reduced in GD patients (Jian et al., 2016b). In a gene array screening from T cells of WT and PGRN KO mice, Chitinase-3 like family members (CHI3L1, CHI3L3, CHI3L4) are up-regulated in PGRN KO mice (Fig. 1A). CHI3L1 was confirmed to have the strongest induction among the three members, especially in spleen (Fig. 1B). In a separate effort to identify proteins that are potentially regulated by PGRN during protein intracellular traffic from ER to lysosome, we isolated cellular organelles from WT and PGRN KO mice spleen tissue, followed by mass spectrum analysis (Fig. 2A). CHI3L1 was identified as the hit most abundantly enriched in PGRN KO mice organelles (Fig. 2B). Clearly, two unbiased screens led to the identification of CHI3L1 as a downstream molecule that is negatively regulated by PGRN. Whether and how CHI3L1 mediates the function of PGRN, especially in Gaucher disease and other lysosomal storage diseases, warrants further investigation.

PGRN null mice develop a cellular phenotype will hallmarks of GD, and CHI3L1 level is significantly increased in this PGRN null GD animal model (Fig. 3). In addition, CHI3L1 expression was reduced following treatment with imiglucerase, recombinant PGRN, or PGRN derivative Pcgin in the PGRN null animal model and fibroblasts obtained from GD patients (Fig. 4), indicating that CHI3L1 level is associated with GD progression. Moreover, CHI3L1 may be a useful biomarker for testing the potential therapeutic effects of newly-developed drug(s) for GD and other lysosomal storage diseases.

We measured serum levels of CHIT1, PGRN, and CHIT3L1 in healthy controls and GD patients. In line with previous reports, serum levels of CHIT1 are significantly higher in GD patients than in healthy controls. Similarly, serum levels of CHI3L1 are also significantly higher (Fig. 5), while serum levels of PGRN are reduced in GD patients, compared with healthy controls (Fig. 5). Surprisingly, correlation analysis among these three factors revealed that PGRN levels are positively correlated with CHI3L1 and CHIT1 in GD patients; there is a weaker correlation between PGRN and CHI3L1 in healthy controls, but no correlation between PGRN and CHIT1 in healthy controls. Although CHI3L1 was isolated as an upregulated gene in PGRN KO mice (Figs. 1–2) and recombinant PGRN negatively regulated CHI3L1 expression in mouse tissues and GD patient fibroblasts (Figs. 3–4), serum levels of PGRN/CHI3L1 are positively correlated in GD patients. These paradoxical findings may result from: 1) that PGRN may be involved in the regulation of the intracellullar and extracellular distribution of CHI3L1 and 2) that other unknown co-factor(s) may affect the expression and/or secretion of CHI3L1, leading to the intriguing correlation between PGRN and CHI3L1 in tissues and body fluids. In PGRN null GD animal models, we measured the intra-cellular levels of CHI3L1 by qPCR and Western-blot, whereas in human samples we measured the serum, i.e. extracellular CHI3L1. In addition, all the GD patient samples used in this study are from individuals that have received treatment. We have shown that CHI3L1 expression was reduced following treatment, and therefore disease management may also contribute to the paradoxical correlation. Furthermore, CHIT1 is a clinical biomarker currently used for diagnosing GD. Interestingly, CHIT1 is also correlated with PGRN in GD patients, which is similar to the correlation between PGRN/CHI3L1. Therefore, it is conceivable that shared mechanisms may contribute to the intriguing relationship among these three molecules. Further studies are needed to thoroughly elucidate the underlying molecular and cellular mechanisms.

In summary, this study identifies CHI3L1 as a previously-unrecognized molecule associated with GD, thus providing a foundation for future discoveries relating to this interesting factor in GD and other lysosomal storage diseases. We have shown that CHI3L1 is upregulated in PGRN null GD model mice, and its expression is correlated with GD progression in both animal models and patient fibroblasts. In addition, CHI3L1 is correlated with PGRN in GD patients, and more importantly, its serum levels are significantly increased in GD patients, as is similar to a current related clinical biomarker CHIT1. Thus, identification and characterization of this new molecule in GD may lead to innovative diagnostic biochemical approaches for LSDs, in particular GD. Additionally, this factor may be also employed as a biomarker for evaluating the therapeutic effects of new treatments for GD. It is also noted that follow-up studies, including those to address the range of expression in untreated patients over degrees of documented clinical severity, and reductions in this marker with clinical response to therapy, are needed to further validate CHI3L1 as a new biomarker of GD and to determine whether CHI3L1 is a better biomarker than those currently employed, in particular CHIT1.

Conflict of Interest

We herein declare that we have no conflict of interest.

Author's Contribution

J. Jian designed and performed experiments, collected and analyzed data, and wrote the paper. Y. Chen, R. Liberti, W. Fu, and W. Hu performed experiments, collected and analyzed data. Rachel Saunders-Pullman provided healthy control samples, G. M. Pastores provided GD patients samples and analyzed data, Y. Chen did statistical analysis, Y. Sun, and G. A. Grabowski did animal studies in *Gba1* D409V/null GD model, analyzed data, and edited manuscript. C.J. Liu designed and supervised this study, analyzed data, and wrote and edited the manuscript. All authors contributed discussions and interpretations.

Acknowledgments

This work was supported partly by NIH research grants 1R01NS103931, R01AR062207, R01AR061484, and a DOD Research Grant W81XWH-16-1-0482. Funders had no role in study design, data collection, data analysis, interpretation, writing of the report.

References

Ahmed, Z., et al., 2010. Accelerated lipofuscinosis and ubiquitination in granulin knockout mice suggest a role for progranulin in successful aging. Am. J. Pathol. 177 (1), 311–324.
Anakwe, O.O., Gerton, G.L., 1990. Acrosome biogenesis begins during meiosis: evidence from the synthesis and distribution of an acrosomal glycoprotein, acrogranin, during guinea pig spermatogenesis. Biol. Reprod. 42 (2), 317–328.
Baker, M., et al., 2006. Mutations in progranulin cause tau-negative frontotemporal dementia linked to chromosome 17. Nature 442 (7105), 916–919.
Baran, A., et al., 2017. Serum YKL-40 as a potential biomarker of inflammation in psoriasis. J. Dermatol. Treat. 1–5.
Barnes, S., et al., 2014. Ubiquitous transgene expression of the glucosylceramide-synthesizing enzyme accelerates glucosylceramide accumulation and storage cells in a Gaucher disease mouse model. PLoS One 9 (12), e116023.
Biegstraaten, M., et al., 2011. A monozygotic twin pair with highly discordant Gaucher phenotypes. Blood Cells Mol. Dis. 46 (1), 39–41.
Boot, R.G., et al., 1998. The human chitotriosidase gene. Nature of inherited enzyme deficiency. J. Biol. Chem. 273 (40), 25680–25685.
Brouwers, N., et al., 2007. Alzheimer and Parkinson diagnoses in progranulin null mutation carriers in an extended founder family. Arch. Neurol. 64 (10), 1436–1446.
Brouwers, N., et al., 2008. Genetic variability in progranulin contributes to risk for clinically diagnosed Alzheimer disease. Neurology 71 (9), 656–664.
Chen, Y., et al., 2017. Tumor-recruited M2 macrophages promote gastric and breast cancer metastasis via M2 macrophage-secreted CHI3L1 protein. J. Hematol. Oncol. 10 (1), 36.
Choy, F.Y., Christensen, C.L., 2016. Progranulin as a novel factor in Gaucher disease. EBioMedicine 13, 13–14.
Cruts, M., et al., 2006. Null mutations in progranulin cause ubiquitin-positive frontotemporal dementia linked to chromosome 17q21. Nature 442 (7105), 920–924.
Di Rosa, M., et al., 2014. Expression of CHI3L1 and CHIT1 in osteoarthritic rat cartilage model. A morphological study. Eur. J. Histochem. 58 (3), 2423.
Di Rosa, M., et al., 2016. Chitinases and immunity: ancestral molecules with new functions. Immunobiology 221 (3), 399–411.
Drugan, C., et al., 2017. Modelling long-term evolution of chitotriosidase in non-neuronopathic Gaucher disease. Scand. J. Clin. Lab. Invest. 77 (4), 275–282.
Elstein, D., et al., 2010. Disease severity in sibling pairs with type 1 Gaucher disease. J. Inherit. Metab. Dis. 33 (1), 79–83.
Erturk, K., et al., 2017. Clinical significance of serum Ykl-40 (Chitinase-3-like-1 protein) as a biomarker in melanoma: an analysis of 112 Turkish patients. Asian Pac. J. Cancer Prev. 18 (5), 1383–1387.
Fu, W., et al., 2016. Foxo4- and Stat3-dependent IL-10 production by progranulin in regulatory T cells restrains inflammatory arthritis. FASEB J. 31 (4), 1354–1367.
Fu, W., et al., 2017. Foxo4- and Stat3-dependent IL-10 production by progranulin in regulatory T cells restrains inflammatory arthritis. FASEB J. 31 (4), 1354–1367.
Futerman, A.H., Platt, F.M., 2017. The metabolism of glucocerebrosides - from 1965 to the present. Mol. Genet. Metab. 120 (1–2), 22–26.
Giraldo, P., et al., 2001. Chitotriosidase genotype and plasma activity in patients type 1 Gaucher's disease and their relatives (carriers and non carriers). Haematologica 86 (9), 977–984.
Grabowski, G.A., 2017. Overview of inflammation in neurometabolic diseases. Semin. Pediatr. Neurol. 24 (3), 207–213.
He, Z., et al., 2003. Progranulin is a mediator of the wound response. Nat. Med. 9 (2), 225–229.
He, C.H., et al., 2013. Chitinase 3-like 1 regulates cellular and tissue responses via IL-13 receptor alpha2. Cell Rep. 4 (4), 830–841.
Hollak, C.E., et al., 1994. Marked elevation of plasma chitotriosidase activity. A novel hallmark of Gaucher disease. J. Clin. Invest. 93 (3), 1288–1292.
Hozumi, H., et al., 2017. Clinical utility of YKL-40 in polymyositis/dermatomyositis-associated interstitial lung disease. J. Rheumatol. 44 (9), 1394–1401.
Hu, X., et al., 2006. IFN-gamma suppresses IL-10 production and synergizes with TLR2 by regulating GSK3 and CREB/AP-1 proteins. Immunity 24 (5), 563–574.
Jian, J., Konopka, J., Liu, C., 2013a. Insights into the role of progranulin in immunity, infection, and inflammation. J. Leukoc. Biol. 93 (2), 199–208.
Jian, J., et al., 2013b. Progranulin directly binds to the CRD2 and CRD3 of TNFR extracellular domains. FEBS Lett. 587 (21), 3428–3436.
Jian, J., et al., 2016a. Progranulin recruits HSP70 to beta-glucocerebrosidase and is therapeutic against Gaucher disease. EBioMedicine 13, 212–224.
Jian, J., et al., 2016b. Association between Progranulin and Gaucher disease. EBioMedicine 11, 127–137.
Jian, J., et al., 2018. Progranulin: a key player in autoimmune diseases. Cytokine 101, 48–55.
Jian, J., Hettinghouse, A., Liu, C.-j., 2017. Progranulin acts as a shared chaperone and regulates multiple lysosomal enzymes. Genes Dis. 4 (3), 125–126.
Junker, N., et al., 2005. Expression of YKL-40 by peritumoral macrophages in human small cell lung cancer. Lung Cancer 48 (2), 223–231.
Kotowicz, B., et al., 2017. Preoperative serum levels of YKL 40 and CA125 as a prognostic indicators in patients with endometrial cancer. Eur. J. Obstet. Gynecol. Reprod. Biol. 215, 141–147.
Kumagai, E., et al., 2016. Serum YKL-40 as a marker of liver fibrosis in patients with non-alcoholic fatty liver disease. Sci. Rep. 6, 35282.
Letuve, S., et al., 2008. YKL-40 is elevated in patients with chronic obstructive pulmonary disease and activates alveolar macrophages. J. Immunol. 181 (7), 5167–5173.
Li, M., et al., 2014. Progranulin is required for proper ER stress response and inhibits ER stress-mediated apoptosis through TNFR2. Cell. Signal. 26 (7), 1539–1548.
Libreros, S., et al., 2012. Induction of proinflammatory mediators by CHI3L1 is reduced by chitin treatment: decreased tumor metastasis in a breast cancer model. Int. J. Cancer 131 (2), 377–386.
Liou, B., et al., 2006. Analyses of variant acid beta-glucosidases: effects of Gaucher disease mutations. J. Biol. Chem. 281 (7), 4242–4253.
Liu, C.J., 2011. Progranulin: a promising therapeutic target for rheumatoid arthritis. FEBS Lett. 585 (23), 3675–3680.
Liu, C.J., Bosch, X., 2012. Progranulin: a growth factor, a novel TNFR ligand and a drug target. Pharmacol. Ther. 133 (1), 124–132.
Liu, C., et al., 2014. Progranulin-derived atsttrin directly binds to TNFRSF25 (DR3) and inhibits TNF-like ligand 1A (TL1A) activity. PLoS One 9 (3), e92743.
Luo, D., et al., 2017. CHI3L1 overexpression is associated with metastasis and is an indicator of poor prognosis in papillary thyroid carcinoma. Cancer Biomark 18 (3), 273–284.
Mundra, J.J., et al., 2016. Progranulin inhibits expression and release of chemokines CXCL9 and CXCL10 in a TNFR1 dependent manner. Sci. Rep. 6, 21115.
Pandey, M.K., et al., 2017. Complement drives glucosylceramide accumulation and tissue inflammation in Gaucher disease. Nature 543 (7643), 108–112.
Plowman, G.D., et al., 1992. The epithelin precursor encodes two proteins with opposing activities on epithelial cell growth. J. Biol. Chem. 267 (18), 13073–13078.
Rathore, A.S., Gupta, R.D., 2015. Chitinases from bacteria to human: properties, applications, and future perspectives. Enzyme Res. 2015, 791907.
Shaker, O.G., Helmy, H.S., 2017. Circulating bone-related markers and YKL-40 versus HER2 and TOPO2a in bone metastatic and nonmetastatic breast cancer: diagnostic implications. Clin. Breast Cancer https://doi.org/10.1016/j.clbc.2017.05.011 (Epub ahead of print, pii: S1526-8209(17)30150-7).
Shantha Kumara, H.M., et al., 2016. Plasma chitinase 3-like 1 is persistently elevated during first month after minimally invasive colorectal cancer resection. World J. Gastrointest Oncol. 8 (8), 607–614.

Shoyab, M., et al., 1990. Epithelins 1 and 2: isolation and characterization of two cysteine-rich growth-modulating proteins. Proc. Natl. Acad. Sci. U. S. A. 87 (20), 7912–7916.
Smith, K.R., et al., 2012. Strikingly different clinicopathological phenotypes determined by progranulin-mutation dosage. Am. J. Hum. Genet. 90 (6), 1102–1107.
Tang, W., et al., 2011. The growth factor progranulin binds to TNF receptors and is therapeutic against inflammatory arthritis in mice. Science 332 (6028), 478–484.
Thurner, L., et al., 2013a. Progranulin antibodies in autoimmune diseases. J. Autoimmun. 42, 29–38.
Thurner, L., et al., 2013b. Progranulin antibodies entertain a proinflammatory environment in a subgroup of patients with psoriatic arthritis. Arthritis Res. Ther. 15 (6), R211.
Thurner, L., et al., 2014. Proinflammatory progranulin antibodies in inflammatory bowel diseases. Dig. Dis. Sci. 59 (8), 1733–1742.
Thurner, L., et al., 2015. The molecular basis for development of proinflammatory autoantibodies to progranulin. J. Autoimmun. 61, 17–28.
Tian, Q.Y., Zhao, Y.P., Liu, C.J., 2012. Modified yeast-two-hybrid system to identify proteins interacting with the growth factor progranulin. J. Visual. Exp. 59.
Tian, Q., Zhao, S., Liu, C., 2014. A solid-phase assay for studying direct binding of progranulin to TNFR and progranulin antagonism of TNF/TNFR interactions. Methods Mol. Biol. 1155, 163–172.
van Dussen, L., et al., 2014. Value of plasma chitotriosidase to assess non-neuronopathic Gaucher disease severity and progression in the era of enzyme replacement therapy. J. Inherit. Metab. Dis. 37 (6), 991–1001.
Wajner, A., et al., 2004. Biochemical characterization of chitotriosidase enzyme: comparison between normal individuals and patients with Gaucher and with Niemann-pick diseases. Clin. Biochem. 37 (10), 893–897.
Wan, G., et al., 2017. Elevated YKL-40 expression is associated with a poor prognosis in breast cancer patients. Oncotarget 8 (3), 5382–5391.
Wei, F., et al., 2014a. Progranulin facilitates conversion and function of regulatory T cells under inflammatory conditions. PLoS One 9 (11), e112110.
Wei, F., et al., 2014b. PGRN protects against colitis progression in mice in an IL-10 and TNFR2 dependent manner. Sci. Rep. 4, 7023.
Wei, J., Hettinghouse, A., Liu, C., 2016. The role of progranulin in arthritis. Ann. N. Y. Acad. Sci. 1383 (1), 5–20.
Williams, A., et al., 2016. Review: novel insights into tumor necrosis factor receptor, death receptor 3, and progranulin pathways in arthritis and bone remodeling. Arthritis Rheum. 68 (12), 2845–2856.
Xu, Y.H., et al., 2011. Global gene expression profile progression in Gaucher disease mouse models. BMC Genomics 12, 20.
Xu, T., et al., 2017. YKL-40 is a novel biomarker for predicting hypertension incidence among prehypertensive subjects: a population-based nested case-control study in China. Clin. Chim. Acta 472, 146–150.
Zanocco-Marani, T., et al., 1999. Biological activities and signaling pathways of the granulin/epithelin precursor. Cancer Res. 59 (20), 5331–5340.
Zhao, C., Bateman, A., 2015. Progranulin protects against the tissue damage of acute ischaemic stroke. Brain 138 (Pt 7), 1770–1773.
Zhao, Y.P., Tian, Q.Y., Liu, C.J., 2013a. Progranulin deficiency exaggerates, whereas progranulin-derived Atsttrin attenuates, severity of dermatitis in mice. FEBS Lett. 587 (12), 1805–1810.
Zhao, Y.P., et al., 2013b. The promotion of bone healing by progranulin, a downstream molecule of BMP-2, through interacting with TNF/TNFR signaling. Biomaterials 34 (27), 6412–6421.
Zhao, Y.P., et al., 2015. Progranulin protects against osteoarthritis through interacting with TNF-alpha and beta-catenin signalling. Ann. Rheum. Dis. 74 (12), 2244–2253.
Zhou, J., et al., 1993. Purification of an autocrine growth factor homologous with mouse epithelin precursor from a highly tumorigenic cell line. J. Biol. Chem. 268 (15), 10863–10869.